JOURNAL OF MAGNETIC RESONANCE **127,** 173–183 (1997)
ARTICLE NO. MN971195

Modeling NMR Lineshapes Using Logspline Density Functions

Jonathan Raz,* Erik J. Fernandez,† and John Gillespie‡

*Department of Biostatistics, School of Public Health, University of Michigan, Ann Arbor, Michigan 48109-2029; †Department of Chemical Engineering, University of Virginia, Charlottesville, Virginia 22903; and ‡Department of Mathematics and Statistics, University of Michigan, Dearborn, Michigan 48128-1491

Received November 20, 1996; revised May 19, 1997

Distortions in the FID and spin echo due to magnetic field inhomogeneity are proved to have a representation as the characteristic function of some probability distribution. In the special case that the distribution is Cauchy, the model reduces to the conventional Lorentzian model. A more general and flexible representation is presented using the Fourier transform of a logspline density. An algorithm for fitting the model is described, the performance of the model and algorithm is investigated in applications to real and simulated data sets, and the logspline approach is compared to a previous Hermitian spline approach and to the Lorentzian model. The logspline model is more parsimonious than the Hermitian spline model, provides a better fit to real data, and is much less biased than the Lorentzian model.

INTRODUCTION

In a homogeneous magnetic field, the free induction decay is the sum of exponentially decaying complex exponentials, and the spectral peaks have a perfect Lorentzian form with widths proportional to $1/T_2$. In practical applications, magnetic field inhomogeneity shortens the observed decay time, thus broadening spectral peaks. Furthermore, in an inhomogeneous field the decay is not necessarily exponential, so the peaks depart from the Lorentzian shape.

Many previous authors have suggested fitting NMR signals in the time or frequency domain by an exponential decay (Lorentzian) model with a relaxation time denoted by T_2^*, where the asterisk indicates the reduction due to inhomogeneity (*1–5*). These models will lead to biased estimates of amplitudes if the true decay is not exponential and the spectral peaks overlap. Estimates of the true values of T_2 from multiple spin echoes (where a separate T_2^* model is fitted to each of the spin echoes) also will be biased.

The HOGWASH (*6*) and QUALITY (*7*) methods convert nonexponential decay to exponential decay under the assumption that all components are distorted by the same multiplicative function. HOGWASH requires an isolated spectral peak, while QUALITY requires a high signal-to-noise ratio (SNR) reference signal with known (or precisely estimated) frequency, phase, and decay rate.

Webb, Spielman, and Macovski (*8*) proposed mapping the field inhomogeneity and using this map to correct observed NMR signals, while Provencher (*9*) directly modeled the distortions by an arbitrary smooth function in the frequency domain. Webb, Collins, and Leach (*10*) represented spectral peaks as the sum of Lorentzian ''spexels'' selected using a stochastic algorithm.

Raz, Chenevert, and Fernandez (*11*), who we cite as RCF in the following, gave a heuristic justification for representing the distorting function as proportional to a probability density function in the frequency domain and as proportional to a characteristic function (the Fourier transform of a probability density function) in the time domain. In this article, we prove that the characteristic function representation is correct under very general conditions.

RCF approximated the complex-valued distorting function in the time domain by two regression splines, one constrained to be an even function and the other to be an odd function, so that the resulting complex-valued function was constrained to be Hermitian. The primary disadvantage of this approach is that the Hermitian spline does not include the more restrictive constraint that a characteristic function be nonnegative definite. A secondary disadvantage is that in typical NMR data sets the phases of the components are constrained to vary linearly with the frequency, and the Hermitian spline model makes it difficult to enforce this constraint. A third limitation of the Hermitian spline model is that it requires very precise knowledge of the echo time τ; RCF performed a grid search over values of τ in fitting the model.

As an alternative to the Hermitian spline model, we propose a flexible model in which the distorting function is proportional to a logspline density function in the frequency domain and thus constrained to be nonnegative definite in the time domain. The linear-phase constraint is enforced as a natural feature of the model, and any errors in the prespecified value of τ are absorbed into the phase parameter.

Like many previous authors (*6–8*), we assume a time-domain model in which the sum of exponentially decaying complex exponentials is multiplied by the distorting function

1090-7807/97 $25.00

that represents inhomogeneity effects. In contrast to the approach of Webb, Spielman, and Macovski (*8*), our method does not require additional mapping scans, and does include estimation of the true value of T_2 as part of the analysis.

In the next two sections, we specify our logspline model of the FID and spin echo. Then we describe maximum likelihood estimation of the model parameters. We report the results of applications of the logspline model to real and simulated spin echoes, with an emphasis on estimation of T_2, and we compare the logspline model to the Hermitian spline model of RCF and the conventional Lorentzian model.

MODELS FOR THE FID AND SPIN ECHO UNDER HOMOGENEOUS AND INHOMOGENEOUS MAGNETIC FIELDS

In this section, we first describe an idealized model for the FID under a homogeneous magnetic field and then define a more realistic model that includes a function representing inhomogeneity effects, and we prove that this function is proportional to the characteristic function of an unknown probability distribution. Then we give the extension of the model to spin-echo signals.

Let $Y(t_j)$ denote the complex-valued FID at time t_j ($j = 1, \ldots, u$ with the t_j equally spaced and $t_1 = 0$ denoting the time of the excitation pulse), and let $N(t_j)$ denote a complex-valued Gaussian white-noise process. In a homogeneous magnetic field, the digitized FID will have the form

$$Y(t_j) = \sum_{k=1}^{K} \alpha_k \exp[-\beta_k t_j + i\omega_k(t_j + \phi)] + N(t_j), \quad j = 1, \ldots, u, \qquad [1]$$

where α_k is the amplitude of component k, β_k is the decay rate ($1/T_2$), ω_k is the frequency, and $\phi\omega_k$ is the phase. The phase term arises from imperfect knowledge of the relationship between the start of data acquisition and the start of the NMR signal.

Magnetic field inhomogeneity causes the frequency ω_k to vary among the nuclei in the object. De Graaf *et al.* (*7*), Webb, Spielman, and Macovski (*8*), and others assumed that B_0 inhomogeneity has the same effect on every spectral component. Under this assumption we may replace ω_k by $\omega_k + \Delta\omega(\mathbf{r})$, where $\mathbf{r} = (r_1, r_2, r_3)$ is a vector of coordinates in three-dimensional space, and $\Delta\omega(\mathbf{r})$ is the deviation of the true frequency at spatial location $\mathbf{r}$ from the average frequency. Then the FID results from integrating over the entire excited volume (*7*),

$$Y(t_j) = \psi(t_j + \phi) \sum_{k=1}^{K} \alpha_k \times \exp[-\beta_k t_j + i\omega_k(t_j + \phi)] + N(t_j), \qquad [2]$$

where, with V denoting the excited volume,

$$\psi(t) = \int_V e^{i\Delta\omega(\mathbf{r})t} dr_1 dr_2 dr_3. \qquad [3]$$

Webb, Spielman, and Macovski (*8*) proposed measuring a discretized version of $\Delta\omega(\mathbf{r})$, and thus computing an approximation to $\psi(t)$.

We now show that the distorting function $\psi(t)$ is proportional to a characteristic function.

THEOREM. *Let V be a bounded Lebesgue measurable subset of $\mathbb{R}^3$, let $\Delta\omega(\mathbf{r})$ be a Lebesgue measurable function on V, and define $\psi(t)$ by Eq. [3]. Then there exists a cumulative distribution function F such that*

$$\psi(t) \propto \int e^{ixt} dF(x), \qquad [4]$$

that is, such that $\psi(t)$ is proportional to the characteristic function of F.

Proof. Let $|V| = \int_V dr_1 dr_2 dr_3$. Write $g(r_1, r_2, r_3) = \Delta\omega(\mathbf{r})$. Let (U_1, U_2, U_3) be a random vector with support V and constant density $1/|V|$. Define the random variable $W = g(U_1, U_2, U_3)$; let F be its cumulative distribution function and let $\psi_F(t)$ be its characteristic function. We can also write this characteristic function in the form

$$\psi_F(t) = E\{\exp[itg(U_1, U_2, U_3)]\} = (1/|V|) \int_V \exp[itg(u_1, u_2, u_3)] du_1 du_2 du_3, \qquad [5]$$

where $E(U)$ denotes the expectation of the random variable U. The right-hand integral is by definition $\psi(t)$, so we have shown that $\psi(t) = |V|\psi_F(t)$; that is, $\psi(t)$ is proportional to the characteristic function of F.

Necessary and sufficient conditions for a function $\psi(t)$ to be a characteristic function are that it be nonnegative definite and that $\psi(0) = 1$ (*12*). Since $\psi(t)$ is nonnegative definite, it is necessarily Hermitian; that is, the real part is an even function and the imaginary part is an odd function. RCF approximated $\psi(t)$ by a regression spline that was constrained to be Hermitian, but not necessarily nonnegative definite.

Two simple models that have been discussed in the NMR literature are special cases of [2] with $\psi(t)$ defined to be a characteristic function. If F is a median zero Cauchy distribution, then

$$\psi(t) = e^{-\gamma|t|}, \quad \gamma > 0. \qquad [6]$$

If we assume that $\phi > 0$, let $\beta_k^* = \beta_k + \gamma$, $T_{2k}^* = 1/\beta_k^*$,

and $\alpha_k^* = \exp(-\gamma\phi)\alpha$, then Eq. [2] with ψ defined by Eq. [6] becomes

$$Y(t_j) = \sum_{k=1}^{K} \alpha_k^* \exp[-t_j/T_{2k}^* + i\omega_k(t_j + \phi)] + N(t_j). \quad [7]$$

This is the conventional Lorentzian model with T_2^* replacing T_2 (*1–5*).

If F is a mean zero normal distribution, then

$$\psi(t) = e^{-\gamma t^2}, \quad \gamma > 0, \quad [8]$$

leading to a model suggested by Barkhuijsen, de Beer, and van Ormondt (*13*).

When $Y(t_j)$ is a spin-echo signal, rather than an FID, then the model defined by Eq. [2] becomes

$$Y(t_j) = \psi(t_j - \tau + \phi) \sum_{k=1}^{K} \alpha_k \times \exp[-\beta_k t_j + i\omega_k(t_j - \tau + \phi)] + N(t_j), \quad [9]$$

where t_j denotes time from the excitation pulse and τ is the echo time.

Combining Eqs. [9] and [6], we see that the Lorentzian model of the spin echo has the form

$$Y(t_j) = \begin{cases} e^{\gamma(\tau-\phi)} \sum_{k=1}^{K} \alpha_k \exp[-(\beta_k + \gamma)t_j \\ \quad + i\omega_k(t_j + \phi)] + N(t_j), \quad t_j \geq \tau - \phi \\ e^{-\gamma(\tau-\phi)} \sum_{k=1}^{K} \alpha_k \exp[-(\beta_k - \gamma)t_j \\ \quad + i\omega_k(t_j + \phi)] + N(t_j), \quad t_j < \tau - \phi. \end{cases} \quad [10]$$

When multiple spin-echo data sets are acquired at distinct echo times in repeated experiments, each using a single excitation pulse and single refocusing pulse, we assume a model of the form

$$Y_s(t_{js}) = \psi(t_{js} - \tau_s + \phi_s) \sum_{k=1}^{K} \alpha_k \times \exp[-\beta_k t_{js} + i\omega_k(t_{js} - \tau_s + \phi_s)] + N_s(t_{js}), \quad s = 1, \ldots, S, j = 1, \ldots, u_s, \quad [11]$$

where $Y_s(t_{js})$ is the complex-valued signal acquired at times t_{js} ($j = 1, \ldots, u_s$) in spin-echo data set s, τ_s is the echo time in data set s, ϕ_s is a factor giving the phase in data set s, $N_s(t)$ is the noise process, and S is the number of spin-echo data sets.

Investigators typically estimate the values of T_2 from multiple spin-echo data sets acquired at distinct echo times. However, it is theoretically possible to estimate the decay rates $\beta_1, \ldots, \beta_K$ (and thus the values of T_2, which are their reciprocals) from a single spin echo, since ψ in model [9] is a Hermitian function centered at $t = \tau - \phi$, while the true spin–spin relaxation is centered at $t = 0$.

LOGSPLINE REPRESENTATION OF CHARACTERISTIC FUNCTIONS

The characteristic function representation of ψ suggests a wide range of parametric models, such as the simple ones derived by assuming that F is Cauchy or normal. However, the functional form of ψ is typically unknown, and it will vary among NMR data sets. This suggests that we should develop a flexible and parsimonious representation of an arbitrary characteristic function, insert this representation for ψ in model [9] or [11], and fit this model to spin-echo data.

Stone and Koo (*14*), Kooperberg and Stone (*15*), and others suggested estimating unknown densities by fitting a logspline model, which is a simple and flexible representation of an arbitrary density function. We suggest representing an arbitrary characteristic function by the Fourier transform of a logspline density function. Let $B_1(\cdot), \ldots, B_q(\cdot)$ be B-spline basis functions (*16*). B-spline basis functions span the space of piecewise polynomials with continuity constraints at the values at which the polynomials are joined. The join points are called ''knots.''

Let $\boldsymbol{\xi} = (\xi_1, \ldots, \xi_q)^T$ be a vector of coefficients for the q B-splines. Then the logspline representation of $\psi(t)$ has the form

$$\psi(t; \boldsymbol{\xi}) = \int e^{ixt} f(x; \boldsymbol{\xi}) dx, \quad [12]$$

where the logspline density is

$$f(x; \boldsymbol{\xi}) = [1/c(\boldsymbol{\xi})] \exp[\sum_{m=1}^{q} \xi_m B_m(x)] \quad [13]$$

with normalizing constant

$$c(\boldsymbol{\xi}) = \int \exp[\sum_{m=1}^{q} \xi_m B_m(x)] dx. \quad [14]$$

These integrals can be evaluated analytically if the B_m are basis functions for linear splines, but not if they are higher-order spline basis functions. However, Fourier integrals can be closely approximated using the fast Fourier transform (FFT) with oversampling and an appropriate tapering function (*17*). We approximated the integral in [12] by oversampling by a factor of 2 and applying a trapezoidal taper. The endpoint corrections given by Press *et al.* (*17*) were

unnecessary, since the estimated logspline density functions decayed to very close to numerical zero near the endpoints. If this were not true, it would mean that the magnetic field inhomogeneity was so severe that peaks in the NMR spectrum would be blurred across the entire frequency band.

The normalizing constant $c(\boldsymbol{\xi})$ could be absorbed into the amplitudes α_k in Eqs. [2], [9], and [11] but this leads to numerical difficulties and should be avoided. Instead, we represent $c(\boldsymbol{\xi})$ by the discretized form:

$$c(\boldsymbol{\xi}) = \sum_l \exp[\sum_{m=1}^{q} \xi_m B_m(x_l)]. \qquad [15]$$

If necessary for preventing numerical underflows or overflows, any constant may be multiplied by $c(\boldsymbol{\xi})$. Since $\psi(t)$ is proportional but not equal to a characteristic function, there is no need to accurately approximate the normalizing constant; the discretized $c(\boldsymbol{\xi})$ is included in the model for numerical stability. (But note that it is a function of the unknown parameter vector $\boldsymbol{\xi}$, which is updated in the iterative fitting procedure described below.)

We refer to model [9] or model [11] with $\psi(t)$ defined by [12] as the logspline model of the spin echo. Note that the lineshape implied by this model is the convolution of the logspline density function with a Lorentzian function [the Fourier transform of $\exp(-\beta_k t)$].

We found that quadratic splines (piecewise quadratic polynomials) performed better in practice than linear or cubic splines. A potential advantage of the quadratic spline is that it can be considered a generalization of the normal distribution, which was used in a model of NMR spectra suggested by Barkhuijsen *et al.* (*13*). A set of q quadratic B-spline basis functions defines a piecewise quadratic polynomial with $q - 2$ knots.

When $\psi(t)$ in model [9] or [11] is defined by Eq. [12], the model is not identifiable, since adding a constant to each frequency ω_k is equivalent to shifting the location of the density f. For this reason, we treat one of the frequencies as a known constant when fitting the model. Identifiability considerations also require that the spline function have zero intercept; this can be achieved by eliminating the first basis function. We generated discrete time B-spline basis functions using the function `bs( )` in the S-plus language for statistical analysis and graphics (*18*). By default, this function assumes zero intercept (*18*).

Model [2] specifies that $\psi(t)$ be evaluated at $t_j + \phi$ rather than at the time points t_j. This is achieved by defining $g_\phi(x; \boldsymbol{\xi}) = e^{ix\phi} f(x; \boldsymbol{\xi})$ and writing the Fourier integral as

$$\psi(t + \phi; \boldsymbol{\xi}) = \int e^{ixt} g_\phi(x; \boldsymbol{\xi}) dx. \qquad [16]$$

This integral is approximated by evaluating $g_\phi(x; \boldsymbol{\xi})$ at discrete values of x and then applying the FFT and taper.

Kooperberg and Stone (*15*) gave recommended values for the number of knots as a function of sample size, but their procedure does not apply to nonlinear regression models such as Eq. [2] with ψ defined in terms of a fixed knot logspline. However, RCF found that model selection criteria such as the Akaiki Information Criterion (AIC) and the Schwartz Bayesian Criterion (SBC) performed well in selecting the number of knots in the Hermitian spline model, and we expect that they would perform well in the logspline model. The phantom data used in our study had a very high signal-to-noise ratio (greater than 4000:1), so we selected the number of knots as the minimum number that gave a nearly perfect fit.

Given the number of knots, we specify the knot locations using the following procedure. We always put knots at the points -1, 0, 1, since the top of the spectral peak is very important in determining the shape of the time-domain function $\psi(t)$. We obtain a preliminary estimate of $f(x)$ with additional knots symmetrically arranged around 0. Placement of these knots can be determined by inspection of the observed spectrum of $\exp(\beta t) y(t)$, where β is set equal to a preliminary estimate of the decay rate of one of the components. For the final estimate, we place knots at equally spaced quantiles of the preliminary estimate of $f(x)$, with the first knot at the ϵ quantile and the last at the $1 - \epsilon$ quantile, where ϵ is 0.01 for a small number of knots and 0.005 or 0.001 for a large number of knots. In some applications, prior knowledge will be available that can be helpful in choosing knot locations. For example, the spectrum might show two peaks at frequencies for which only a single component is known to exist, indicating that $f(x)$ is bimodal. In such a case, the knots can be chosen with the aid of a plot of the spectrum of $\exp(\beta t) y(t)$.

MAXIMUM LIKELIHOOD ESTIMATION OF MODEL PARAMETERS

Given specified values of the echo time τ and the B-spline basis functions, the logspline model is a fully specified parametric model in terms of the parameter vectors $\boldsymbol{\alpha} = (\alpha_1, \ldots, \alpha_K)^T$, $\boldsymbol{\xi}$, and $\boldsymbol{\theta} = (\beta_1, \ldots, \beta_K, \omega_2, \ldots, \omega_K, \phi)^T$, where ω_1 is set equal to its starting value and treated as a known constant. Under the assumption that the noise process $N(t_j)$ is complex-valued Gaussian white noise, the maximum likelihood estimates minimize the objective function

$$L(\boldsymbol{\alpha}, \boldsymbol{\xi}, \boldsymbol{\theta}) = \sum_{j=1}^{u} |y(t_j) - \psi(t_j - \tau + \phi; \boldsymbol{\xi}) \times \sum_{k=1}^{K} \alpha_k \exp[-\beta_k t_j + i\omega_k (t_j - \tau + \phi)]|^2. \qquad [17]$$

Given $\boldsymbol{\xi}$ and $\boldsymbol{\theta}$, the model is linear in the vector $\boldsymbol{\alpha}$. The partial linearity may be exploited by ''concentrating out'' $\boldsymbol{\alpha}$

in a ''concentrated'' or ''profile'' likelihood (*19*); algorithms based on this property have been applied under the name ''Variable Projection'' to NMR data (*4, 5*). We use a related but simpler algorithm that is similar to several procedures described by Seber and Wild (*19*). Given starting values, we alternate a Levenberg–Marquardt update of $\boldsymbol{\theta}$ and $\boldsymbol{\xi}$ with a least-squares computation of $\boldsymbol{\alpha}$ given the current values of $\boldsymbol{\theta}$ and $\boldsymbol{\xi}$. This algorithm is the same as that used by RCF, except that here $\boldsymbol{\alpha}$ is treated as the linear parameter, while in RCF the vector of Hermitian spline coefficients was the linear parameter.

The Levenberg–Marquardt step requires the first derivative of the expectation of $Y(t)$ with respect to the parameters, and thus the first derivative of $\psi(t + \phi; \boldsymbol{\xi})$ with respect to $\boldsymbol{\xi}$ and ϕ. These derivatives are approximated by taking the derivatives under the integral in Eq. [16] and then approximating the resulting Fourier integral. The derivative of $f(x; \boldsymbol{\xi})$ is evaluated by taking derivatives of both the numerator and the denominator in Eq. [13] with $c(\boldsymbol{\xi})$ defined by Eq. [15]. Each Levenberg–Marquardt update requires $q + 2$ FFTs, one to approximate $\psi(t; \boldsymbol{\xi})$, one to approximate its derivative with respect to ϕ, and q to approximate its derivatives with respect to $\boldsymbol{\xi}$.

We also implemented an algorithm that fits the Lorentzian model [10] to a time-domain spin-echo signal. The model and algorithm include the linear-phase assumption and thus differ slightly from those used by RCF.

The algorithm for fitting model [11] to multiple spin-echo data sets acquired at distinct echo times is the same as that for single spin-echo data sets, except that a separate phase parameter ϕ_s is estimated for each echo.

When fitting the logspline model to spin echoes with two poorly separated spectral peaks, the optimization algorithm occasionally converges to a local minimum in which $f(x)$ is bimodal, and one of the modes of $f(x)$ explains part of one of the peaks. Refitting with different knot locations and/or a different number of knots solved this problem when we encountered it. In such cases, the model based on the local minimum had a noticeably poor fit, and the true minimum gave much smaller values of the objective function. We suspect that this problem also could arise in very noisy data with more than two peaks if all the peaks are arranged in pairs.

We define the starting values for the frequencies $\omega_1, \ldots, \omega_K$ to be the peak frequencies in the magnitude spectrum. For identifiability, we treat the frequency corresponding to the highest peak as a known constant in the iterative algorithm. To define starting values for the phase parameter ϕ, we compute the complex demodulate (*20*) of the data at these peak frequencies, and compute ϕ from the argument of the demodulate of the highest peak, remembering that the phase is actually $\phi\omega_k$ rather than ϕ itself. For $k = 1, \ldots, K$, we use weighted least squares to fit $-\beta_k t - \gamma|t - \tau + \phi|$ to the logarithm of the magnitude of the kth demodulate to obtain a starting value for the decay parameter β_k. We define a preliminary estimate of $\psi(t)$ to be equal to $e^{-\gamma|t-\tau|}$ with γ set equal to the value computed from the demodulate of the highest peak. Then we compute amplitude parameters $\alpha_1, \ldots, \alpha_K$ by ordinary least squares. We compute starting values for $\boldsymbol{\xi}$ by a linear fit of the B-spline (with an intercept) to $-\gamma|t - \tau + \phi|$. The estimate of the intercept coefficient is not used, but it must be included in the model to account for the normalizing constant in the logspline density.

The value of τ can be computed from the timing of the data acquisition and is not updated in the iterative fitting algorithm. Any error in τ will be absorbed into the estimate of ϕ. If the computed τ is far from the true value (so the estimated value of ϕ is large in absolute value) then refitting with an improved value of τ based on the estimate of ϕ may give a better fit.

In fitting multiple spin-echo data sets, we compute starting values for the decay parameters β_k from the peak heights of the spectra.

APPLICATIONS TO PHANTOM DATA

We compared the fit of the logspline model to that of the Lorentzian model and the Hermitian spline model of RCF in applications to hydrogen (^{1}H) spin echoes acquired from six different chemical samples (''phantoms''). We also used these applications to demonstrate the feasibility of estimating T_2 from a single spin echo.

The first set of three phantoms, which we denote by W5, W10, and W20, contained distilled water with 50, 100, or 200 micromolar (μM) concentration of manganese chloride ($MnCl_2$) in solution. The T_2 of the hydrogen nuclei (protons) in the water decreases with increasing concentration of $MnCl_2$. There is a single component in echoes acquired from these phantoms ($K = 1$). The second set of two phantoms, which we denote by D5 and D10, contained dioxane ($C_4H_8O_2$) mixed with a solution of 50 or 100 μM $MnCl_2$ in distilled water. The W and D sets of water/manganese solutions were prepared at different times and probably contained slightly different molar concentrations of manganese, even when the nominal concentrations were the same. The final phantom, which we denote by MeOH, contained pure methanol (CH_3OH). Echoes acquired from the D5, D10, and MeOH phantoms have two components ($K = 2$). All signals comprised $u = 1022$ time points. (The data included 1024 points but the first two contained artifacts.) Spin echoes were acquired from the W5 phantom with nominal echo times $\tau = 50, 100, 200$ ms, and were digitized at 40,000 hertz. Spin echoes were acquired from the other five phantoms with nominal echo times $\tau = 50, 100, 200, 300$ ms, and were digitized at 20,000 hertz.

Acquisition was performed by a 2 T/31 cm Omega CSI spectrometer (Bruker Instruments; formerly GE NMR instruments, Fremont, CA), using a 14 cm birdcage-design

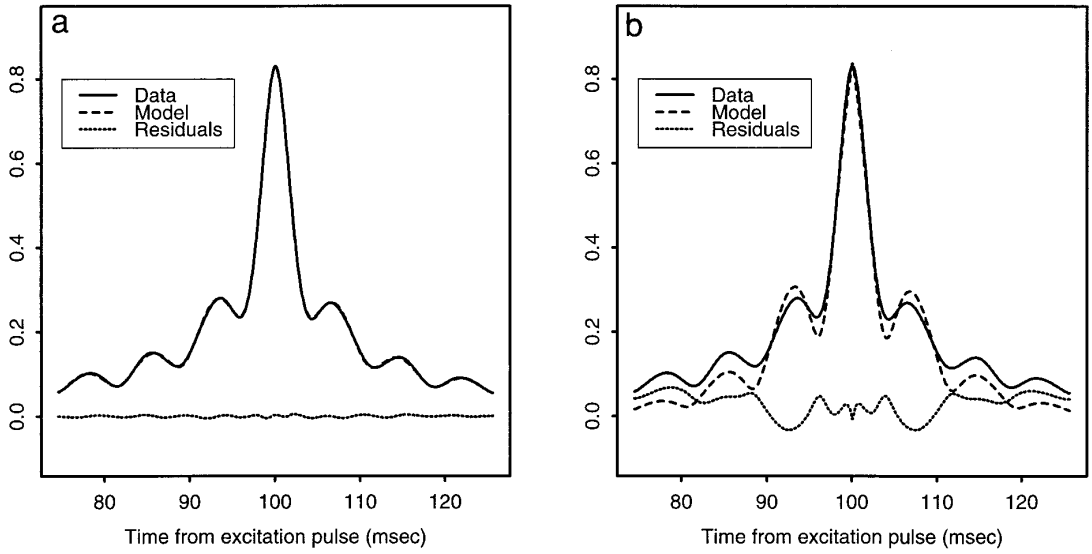

FIG. 1. Comparison of the modulus of two fitted time-domain models with the modulus of the spin echo acquired from a phantom containing methanol. (a) Logspline model. (b) Lorentzian model. In both plots, the solid line indicates the data, the dashed line the model, and the dotted line the difference between the data and model (residuals). The logspline model nearly interpolates the data, while the Lorentzian model exhibits serious bias.

transmit and receive RF coil. The pulse sequence was a 90°—180°—acquisition. All acquisitions were performed with only partial optimization of the shimming, so that considerable inhomogeneity was present. The signals were averages of 32 phase-cycled (*21*) acquisitions following 8 dummy scans, giving spin echoes with very high SNR. The phase cycling is essential for estimation of T_2 from a single spin echo, since the effects of an imperfect refocusing pulse can obscure the subtle T_2 effects.

RCF reported estimated values of T_2 for these data sets based on the Hermitian spline model and the Lorentzian model without the assumption of linear phase. The Hermitian spline model included a total of 16 spline coefficients, corresponding to 6 knots (which are used for both the real and the imaginary parts of the Hermitian spline function). The total number of parameters in the Hermitian spline model was 23.

We fitted both the logspline model and the Lorentzian model with linear phase to each of the single spin-echo data sets. The logspline models had 7, 11, or 15 knots (9, 13, or

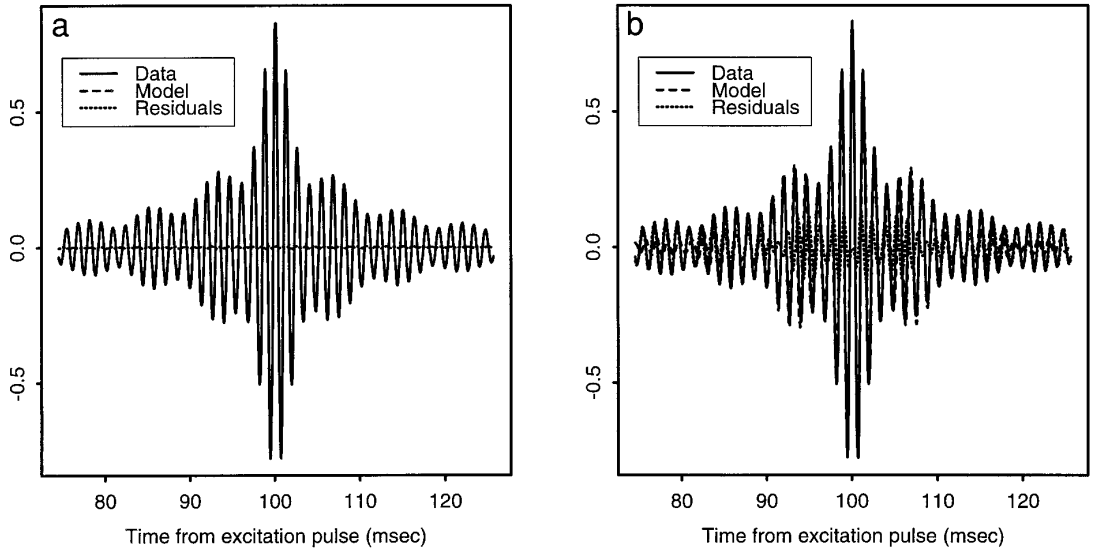

FIG. 2. Comparison of the real part of two fitted time-domain models with the real part of the spin echo acquired from a phantom containing methanol. (a) Logspline model. (b) Lorentzian model.

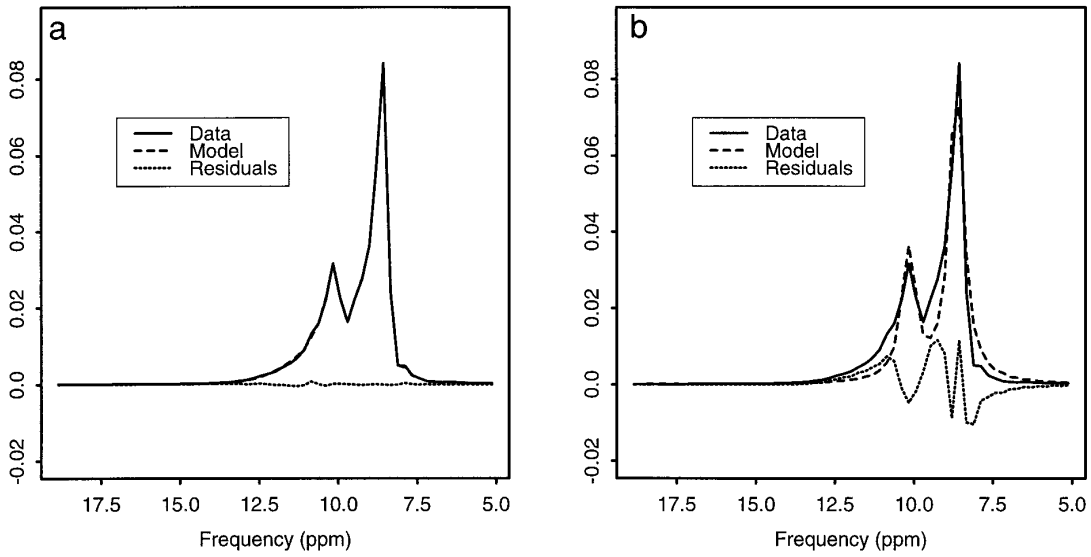

FIG. 3. Comparison of the spectrum (modulus of the Fourier transform) of two fitted time-domain models with the spectrum of the spin echo acquired from a phantom containing methanol. (a) Logspline model. (b) Lorentzian model.

17 spline coefficients; 15, 19, or 23 total parameters). When fitting the 7- and 15-knot models, the iterative algorithm converged to excellent fits in most analyses, but to obvious local minima for a few of the echoes, while the 11-knot models seemed to give excellent fits in all cases. Furthermore, the 11-knot models gave considerably smaller values of the objective function than the 7-knot models, but the 15-knot models at best provided little additional improvement, and they generally gave point estimates close to those from the 11-knot models. For these reasons, we report results only from the 11-knot models.

In all analyses (a total of 23 spin-echo data sets), the fit of the logspline model, as measured by the objective function, was much better than the fit of the Lorentzian model. Furthermore, in 17 of the 23 analyses, the fit of the logspline model was better than that of the Hermitian spline model, even though the 11-knot logspline model is more parsimonious than the 6-knot Hermitian spline model used by RCF. This result suggests that the more restrictive assumptions (nonnegative definite ψ and linear phase) of the logspline model are justified.

Figures 1 and 2 compare the fitted logspline and Lorentzian models to the time-domain signal of a selected spin echo. Figure 3 compares the fitted models to the magnitude spectrum of the spin echo. These figures are very similar to Fig. 3 of RCF, since the error in both the logspline model and the Hermitian spline model of RCF is very small, while the Lorentzian model with or without the linear-phase assumption shows obvious model misspecification. Results for the other echoes are qualitatively similar.

We also computed ''gold standard'' T_2 estimates by fitting model [11] with the logspline or Lorentzian definitions of ψ to all available echoes acquired from a particular phantom (three echoes for the W5 phantom, four for the other five phantoms). These multiecho estimates were almost identical to the Hermitian spline and Lorentzian estimates given by RCF.

Table 1 shows the estimated T_2 values (computed as the reciprocal of the estimated decay rates) of the W20, W10,

TABLE 1
Estimated T_2 (in Milliseconds) of Protons in Three Water Phantoms for Two Inhomogeneity Models[a]

		Inhomogeneity model	
Phantom	τ	Lorentz	Logspline
W20	**All**	**55**	**55**
	50	54	56
	100	54	56
	200	53	55
W10	**All**	**94**	**94**
	50	83	96
	100	82	96
	200	82	98
	300	90	100
W5	**All**	**198**	**196**
	50	189	209
	100	180	210
	200	188	213
	300	202	222

[a] In the column headed τ, the numerical values are for the single-echo estimates, while ''All'' indicates the ''gold standard'' multiecho estimates. These gold standard estimates are highlighted by boldface type.

TABLE 2

Estimated T_2 (in Milliseconds) of Protons in Two Water/Dioxane Phantoms and the Methanol Phantom for Two Inhomogeneity Models[a]

		Inhomogeneity model	
Phantom	τ	Lorentz	Logspline
D10	**All**	**118, 2086**	**107, 1788**
	50	116, 3009	111, 1827
	100	115, 2088	108, 1613
	200	135, 2296	106, 1916
	300	197, 2362	126, 2064
D5	**All**	**200, 2192**	**188, 1859**
	50	205, 3663	194, 1870
	100	192, 1960	191, 1656
	200	214, 2080	199, 1827
	300	215, 3736	185, 2954
MeOH	**All**	**184, 382**	**123, 369**
	50	216, 368	182, 480
	100	407, 378	173, 471
	200	327, 365	139, 436
	300	314, 369	143, 412

[a] In the column headed τ, the numerical values are for the single-echo estimates, while ''All'' indicates the ''gold standard'' multiecho estimates. These gold standard estimates are highlighted by boldface type. For the D10 and D5 phantoms, the first estimate in each pair corresponds to the water component, and the second to the dioxane component. For the MeOH phantom, the first estimate corresponds to the hydroxyl component, and the second to the methyl component.

and W5 phantoms, while Table 2 shows the estimated T_2 values of the D10, D5, and MeOH phantoms. Two estimates, the reciprocals of the estimated β_1 and β_2, are shown for each echo and model in Table 2. For the D10 and D5 phantoms, the T_2 estimates are for water first, and then dioxane. For the MeOH phantom, the estimates are for hydroxyl protons first, followed by methyl protons.

We quantified the agreement between the single-echo and multiecho T_2 estimates using a quantity defined by

$$\rho = \left[1 + \frac{\sum_{b=1}^{B} (x_b - y_b)^2}{\sum_{b=1}^{B} (x_b - x_\cdot)^2} \right]^{-1}, \qquad [18]$$

where $x_1, \ldots, x_B$, are the logarithms of the multiecho gold standard T_2 estimates (boldface type in Table 1 or 2), $x_\cdot = (1/B) \Sigma\, x_b$, and $y_1, \ldots, y_B$ are the logarithms of the single-echo estimates (roman type in Table 1 or 2). The quantity ρ was recently proposed by Roy St. Laurent (personal communication), and is similar to the ''concordance correlation coefficient'' of Lin (*22*). If there is infinite disagreement between x and y, then $\rho = 0$; if x and y are independent and identically distributed Gaussian random variables and B is large, then ρ is approximately $\frac{1}{3}$; if $x_b = y_b$ for $b = 1, \ldots, B$, then $\rho = 1$. When ρ is computed from the logarithms of the T_2 estimates, it is identical to ρ computed from the logarithms of the β_k estimates.

Based on the logarithms of the estimates in Tables 1 and 2 with the logspline multiecho estimates as the gold standard, $\rho = 0.98$ for the logspline single-echo estimates and 0.90 for the Lorentzian single-echo estimates. The performance of the Lorentzian model was even worse in applications to echoes with two components (Table 2, $\rho = 0.86$), while the logspline model showed no difficulty with two components (Table 2, $\rho = 0.98$). This indicates the importance of correctly modeling the inhomogeneity distortions in separating overlapping spectral peaks. The logspline model also agreed more with the Lorentzian multiecho gold standard estimates than did the Lorentzian single-echo estimates ($\rho = 0.99$ vs $\rho = 0.95$).

The Hermitian spline estimates (Tables 1 and 2 in RCF) gave $\rho = 0.98$ when the logspline or Hermitian spline multiecho estimates were the gold standard. Thus, the more parsimonious logspline model gave T_2 estimates that were just as good as those produced by the Hermitian spline model.

APPLICATIONS TO SIMULATED DATA

The applications to phantom data suggested that the logspline model is much better than the Lorentzian model and gives somewhat better fits than the Hermitian spline model while using fewer parameters. However, the phantom data sets were nearly free of noise. To further compare the models, we analyzed simulated data with three different SNRs (infinite, 100, and 10, where SNR was defined as in RCF) and known parameter values as in RCF (except that linear phase was assumed and the phase ϕ was set equal to zero). As in RCF, the simulated ψ function was the characteristic function of a mixture of two stable distributions that are intermediate between the Cauchy and a normal. This function is similar to the estimated ψ functions from the analyses of the phantom data and was not generated from a Lorentzian, Hermitian spline, or logspline model.

For each of two sets of parameter values (based on analyses of the water/dioxane and methanol data sets) and three SNRs, we simulated 100 spin echoes and analyzed them with each of five models: Hermitian spline with 2 or 4 knots (15 or 19 total parameters including 1 amplitude, 2 decay parameters, 2 frequencies, 2 phases, and 8 or 12 spline coefficients), logspline with 7 or 11 knots (15 or 19 total parameters including 2 amplitudes, 2 decay parameters, 1 frequency, 1 phase, and 9 or 13 spline coefficients), and Lorentzian with linear phase (8 parameters). The knot locations for the Hermitian spline were as in RCF, while the knot locations for the logspline were chosen as described under Logspline Representation of Characteristic Functions, using a preliminary fit to the simulated spin echo without noise. Thus, the

TABLE 3

Results of Simulation Study Based on Methanol Data: Estimated Bias of Estimators (as Percentage of True Parameter Value) of Amplitudes (α_k) and Decay Rates (β_k), for Each Signal-to-Noise Ratio (SNR) and Five Inhomogeneity Models (with the Number of Model Parameters in Parentheses)

		Inhomogeneity model				
SNR	Estimator	Hermitian spline (15)	Hermitian spline (19)	Logspline (15)	Logspline (19)	Lorentzian (8)
∞	$\hat{\alpha}_1$	5.6	0.9	2.1	1.0	0.9
	$\hat{\alpha}_2$	7.5	1.0	1.7	0.4	3.3
	$\hat{\beta}_1$	18.2	0.1	16.9	1.3	15.2
	$\hat{\beta}_2$	2.1	0.0	0.7	0.1	8.7
100	$\hat{\alpha}_1$	−5.3	−0.7	−1.9	−0.7	−0.6
	$\hat{\alpha}_2$	−7.5	−1.0	−1.7	−0.4	−3.3
	$\hat{\beta}_1$	−18.0	0.3	−16.6	1.5	−14.9
	$\hat{\beta}_2$	2.3	0.2	−0.4	0.3	8.9
10	$\hat{\alpha}_1$	−5.9	0.2	0.4	1.0	0.3
	$\hat{\alpha}_2$	−6.3	0.3	1.0	1.8	−1.8
	$\hat{\beta}_1$	−26.9	−5.3	−20.4	−5.1	−18.4
	$\hat{\beta}_2$	6.3	4.9	4.2	4.3	14.0

Note. The true parameter values were $\alpha_1 = 0.2981$, $\alpha_2 = 0.8054$, $\beta_1 = 0.004802$ ms^{-1}, $\beta_2 = 0.002216$ ms^{-1}, $\omega_1 = 5.7301$ rad/ms = 10.666 ppm, $\omega_2 = 4.8889$ rad/ms = 9.100 ppm, and $\phi = 0$ ms. The amplitudes are in arbitrary units.

simulations ignored the variability due to empirical selection of knots from a noisy data set.

Tables 3 and 5 give the estimated bias of the estimators of the two amplitudes (α_1 and α_2) and two decay parameters (β_1 and β_2). The estimated bias is expressed as a percentage of the true parameter value. (The second amplitude in the Hermitian spline model is not explicitly modeled; instead, it is derived from the estimated spline function.)

The Hermitian spline results differ slightly from those in RCF because the simulations used different phase parameters and different random number seeds. The Lorentzian results also differ from those in RCF, because the Lorentzian model applied here assumes linear phase, while the Lorentzian model in RCF allowed separate phase parameters for each component.

The two spline models with 19 total parameters gave nearly unbiased estimates and much lower bias than the Lorentzian model, regardless of the SNR (Tables 3 and

TABLE 4

Results of Simulation Study Based on Methanol Data: Estimated Root Mean Square Error of Estimators (as Percentage of True Parameter Value) of Amplitudes (α_k) and Decay Rates (β_k), for Each Signal-to-Noise Ratio (SNR) and Five Inhomogeneity Models (with the Number of Model Parameters in Parentheses)

		Inhomogeneity model				
SNR	Estimator	Hermitian spline (15)	Hermitian spline (19)	Logspline (15)	Logspline (19)	Lorentzian (8)
100	$\hat{\alpha}_1$	5.9	3.1	3.2	3.1	2.6
	$\hat{\alpha}_2$	7.6	1.3	1.9	0.9	3.4
	$\hat{\beta}_1$	18.8	6.3	17.5	6.5	15.9
	$\hat{\beta}_2$	4.4	3.7	3.6	3.7	9.8
10	$\hat{\alpha}_1$	23.7	27.3	24.7	28.7	23.5
	$\hat{\alpha}_2$	9.5	7.6	8.5	19.3	8.1
	$\hat{\beta}_1$	73.2	57.2	54.0	58.0	52.0
	$\hat{\beta}_2$	34.4	33.9	34.3	34.2	38.6

Note. The root mean square for the SNR = ∞ case is equal to the absolute value of the bias given in Table 3. The true parameter values are given in the footnote to Table 3.

TABLE 5

Results of Simulation Study Based on Water/Dioxane Data: Estimated Bias of Estimators (as Percentage of True Parameter Value) of Amplitudes (α_k) and Decay Rates (β_k), for Each Signal-to-Noise Ratio (SNR) and Five Inhomogeneity Models (with the Number of Model Parameters in Parentheses)

		Inhomogeneity model				
SNR	Estimator	Hermitian spline (15)	Hermitian spline (19)	Logspline (15)	Logspline (19)	Lorentzian (8)
∞	$\hat{\alpha}_1$	−5.6	−1.0	−3.1	−0.6	−5.2
	$\hat{\alpha}_2$	−1.4	−1.0	0.4	−0.8	−6.5
	$\hat{\beta}_1$	5.7	0.2	−3.5	0.1	−11.3
	$\hat{\beta}_2$	16.1	0.1	20.9	−1.5	13.2
100	$\hat{\alpha}_1$	−5.7	−1.1	−3.2	−0.6	−5.3
	$\hat{\alpha}_2$	−1.5	−1.0	0.4	−0.8	−6.6
	$\hat{\beta}_1$	5.6	0.0	−3.6	−0.1	−11.4
	$\hat{\beta}_2$	14.6	−1.0	19.7	−2.9	11.7
10	$\hat{\alpha}_1$	−6.0	−1.5	−3.0	0.8	−5.9
	$\hat{\alpha}_2$	−8.2	−0.5	1.5	1.9	−6.0
	$\hat{\beta}_1$	4.4	−1.2	−5.3	−1.0	−12.7
	$\hat{\beta}_2$	14.4	−0.9	17.4	−4.6	11.2

Note. The true parameter values were $\alpha_1 = 0.8607$, $\alpha_2 = 0.465$, $\beta_1 = 0.009277$ ms^{-1}, $\beta_2 = 0.0006119$ ms^{-1}, $\omega_1 = -5.8742$ rad/ms $= -10.935$ ppm, $\omega_2 = -6.3240$ rad/ms $= -11.772$ ppm, and $\phi = 0.0$ ms. The amplitudes are in arbitrary units.

5). With 15 total parameters, the logspline estimators of the amplitudes were nearly unbiased and had less bias than the Hermitian spline estimators with 15 parameters. The Lorentzian model and both 15-parameter spline models gave quite biased estimates of one of the decay parameters (β_1 in Table 3 and β_2 in Table 5) regardless of SNR.

Decreasing bias tends to increase variance, so it is important to compare the root mean square error (RMSE) of the estimators. The square of the RMSE equals the variance plus the squared bias. Tables 4 and 6 give the estimated RMSE as a percentage of the true parameter value. When the SNR was 100, the spline models with 19 total parameters had much lower RMSE than did the Lorentzian model. None of the models had consistently lowest RMSE when the SNR was 10. The logspline model with 15 parameters gave lower RMSE than the Hermitian spline model with the same number of para-

TABLE 6

Results of Simulation Study Based on Water/Dioxane Data: Estimated Root Mean Square Error of Estimators (as Percentage of True Parameter Value) of Amplitudes (α_k) and Decay Rates (β_k), for Each Signal-to-Noise Ratio (SNR) and Five Inhomogeneity Models (with the Number of Model Parameters in Parentheses)

		Inhomogeneity model				
SNR	Estimator	Hermitian spline (15)	Hermitian spline (19)	Logspline (15)	Logspline (19)	Lorentzian (8)
100	$\hat{\alpha}_1$	5.9	1.8	3.5	1.6	5.5
	$\hat{\alpha}_2$	1.9	1.6	1.3	1.4	6.7
	$\hat{\beta}_1$	5.9	1.7	4.0	1.7	11.5
	$\hat{\beta}_2$	24.4	20.0	27.6	20.2	25.5
10	$\hat{\alpha}_1$	14.8	13.4	13.0	13.9	12.4
	$\hat{\alpha}_2$	9.7	9.3	9.5	10.5	11.8
	$\hat{\beta}_1$	17.0	15.0	14.9	14.9	18.1
	$\hat{\beta}_2$	152.1	153.1	149.6	155.9	175.4

Note. The root mean square for the SNR $= \infty$ case is equal to the absolute value of the bias given in Table 5. The true parameter values are given in the footnote to Table 5.

meters, except in the case of β_2 in the water/dioxane simulations (Table 6) and α_1 for the SNR = 10 methanol simulations (Table 4).

As pointed out by RCF, *in vivo* NMR data commonly has much lower SNR than that used here, making estimation of T_2 from a single spin echo impractical. If we had assumed that some of the parameters were known, as in Webb, Spielman, and Macovski (*8*) and Spielman *et al.* (*4*), then we could have compared the models at lower SNRs. We expect that the logspline model would perform very well at moderately low SNR if the T_2 values and possibly other parameters were known. We expect that at very low SNR, a more parsimonious model, such as the Lorentzian model, will have lower RMSE than the logspline model.

DISCUSSION

We have derived a representation of inhomogeneity distortions in NMR time series as characteristic functions, represented these distorting functions by the Fourier transform of a logspline density, and applied the resulting model to real and simulated NMR data. The logspline model is more parsimonious than the Hermitian spline model of RCF and much less biased than the conventional Lorentzian model. Further, the logspline model, unlike the Hermitian spline model, facilitates implementation of a linear-phase assumption, and does not require precise knowledge of the echo time τ.

The Hermitian spline model with few knots resembles a polynomial, which can be quite unlike a characteristic function. The logspline model, in contrast, represents ψ by a characteristic function regardless of the number of knots.

Our choice of B-spline basis functions is only one of many possible choices. We note that a similar method could be constructed by exponentiating any other set of basis functions.

We fitted the logspline model in the time domain, which avoids evaluating convolutions in the frequency domain, but which requires repeated FFTs. An alternative approach would be to fit the logspline model in the frequency domain using a discrete convolution as proposed by Provencher (*9*). This approach would differ from Provencher's in that the distorting function would be represented by a logspline rather than an arbitrary smooth function.

ACKNOWLEDGMENTS

The work of Dr. Raz was supported by National Science Foundation Award DMS-9116730. We gratefully acknowledge the valuable contributions of Thomas Chenevert and James Pipe, who acquired the phantom data; Robert Sharp, who prepared the phantoms; Donald Twieg, who introduced Dr. Raz to many basic concepts of NMR, and particularly to the problems of modeling spin-echo signals; and Andrew Maudsley, Sarah Nelson, Richard Olshen, William Redfearn, and Ronald Thomas, who made helpful suggestions during development of the methodology.

REFERENCES

1. H. Barkhuijsen, R. de Beer, W. M. M. J. Bovée, and D. van Ormondt, *J. Magn. Reson.* **61,** 465 (1985).
2. M. I. Miller and A. S. Greene, *J. Magn. Reson.* **83,** 525 (1989).
3. S. J. Nelson and T. R. Brown, *J. Magn. Reson.* **84,** 95 (1989).
4. D. Spielman, P. Webb, and A. Macovski, *J. Magn. Reson.* **79,** 66 (1988).
5. J. W. C. van der Veen, R. de Beer, P. R. Luyten, and D. van Ormondt, *Magn. Reson. Med.* **6,** 92 (1988).
6. S. J. Davies, C. Bauer, P. Hore, and R. Freeman, *J. Magn. Reson.* **76,** 476 (1988).
7. A. A. de Graaf, J. E. van Dijk, and W. M. M. J. Bovée, *Magn. Reson. Med.* **13,** 343 (1990).
8. P. Webb, D. Spielman, and A. Macovski, *Magn. Reson. Med.* **23,** 1 (1992).
9. S. W. Provencher, *Magn. Reson. Med.* **30,** 672 (1993).
10. S. Webb, D. J. Collins, and M. O. Leach, *NMR Biomed.* **5,** 87 (1992).
11. J. Raz, T. Chenevert, and E. J. Fernandez, *J. Magn. Reson. A* **111,** 137 (1994).
12. E. Lukacs, ''Characteristic Functions,'' 2nd ed., Griffin, London, 1970.
13. H. Barkhuijsen, R. de Beer, and D. van Ormondt, *J. Magn. Reson.* **67,** 371 (1986).
14. C. J. Stone and C.-Y. Koo, *Contemp. Math.* **59,** 1 (1986).
15. C. Kooperberg and C. J. Stone, *Comput. Statist. Data Anal.* **12,** 327 (1991).
16. R. L. Eubank, ''Spline Smoothing and Nonparametric Regression,'' Dekker, New York, 1988.
17. W. H. Press, S. A. Teukolsky, W. T. Vetterling, and B. P. Flannery, ''Numerical Recipes in Fortran,'' 2nd ed., Cambridge Univ. Press, Cambridge, UK, 1992.
18. J. M. Chambers and T. J. Hastie (Eds.), ''Statistical Models in S,'' Wadsworth & Brooks/Cole, Pacific Grove, CA, 1992.
19. G. A. F. Seber and C. J. Wild, ''Nonlinear Regression,'' pp. 657–660, Wiley, New York, 1989.
20. P. Bloomfield, ''Fourier Analysis of Time Series: An Introduction,'' Wiley, New York, 1976.
21. D. I. Hoult and R. E. Richards, *Proc. R. Soc. (London) A* **344,** 311 (1975).
22. L. Lin, *Biometrics* **45,** 255 (1989).